Journal of Hazardous Materials 184 (2010) 533–537

Contents lists available at ScienceDirect

Journal of Hazardous Materials

journal homepage: www.elsevier.com/locate/jhazmat

Enhancement of tributyltin degradation under natural light by N-doped TiO_2 photocatalyst

S. Bangkedphol[a,*], H.E. Keenan[a], C.M. Davidson[b], A. Sakultantimetha[a], W. Sirisaksoontorn[c], A. Songsasen[c]

[a] David Livingstone Centre for Sustainability, Department of Civil Engineering, University of Strathclyde, Glasgow, Scotland G1 1XN, United Kingdom
[b] WestCHEM, Department of Pure and Applied Chemistry, University of Strathclyde, Glasgow, Scotland G1 1XL, United Kingdom
[c] Department of Chemistry and Centre for Innovation in chemistry, Faculty of Science, Kasetsart University, Bangkok 10900, Thailand

ARTICLE INFO

Article history:
Received 25 February 2010
Received in revised form 16 August 2010
Accepted 19 August 2010
Available online 26 August 2010

Keywords:
Tributyltin
N-doped TiO_2
Photocatalytic degradation
Sol–gel

ABSTRACT

Photo-degradation of tributyltin (TBT) has been enhanced by TiO_2 nanoparticles doped with nitrogen (N-doped TiO_2). The N-doped catalyst was prepared by a sol–gel reaction of titanium (IV) tetraisopropoxide with 25% ammonia solution and calcined at various temperatures from 300 to 600 °C. X-ray diffraction results showed that N-doped TiO_2 remained amorphous at 300 °C. At 400 °C the anatase phase occurred then transformed to the rutile phase at 600 °C. The crystallite size calculated from Scherrer's equation was in the range of 16–51 nm which depended on the calcination temperature. N-doped TiO_2 calcined at 400 °C which contained 0.054% nitrogen, demonstrated the highest photocatalytic degradation of TBT at 28% in 3 h under natural light when compared with undoped TiO_2 and commercial photocatalyst, P25–TiO_2 which gave 14.8 and 18% conversion, respectively.

1. Introduction

To prevent fouling of ship's hulls by small organisms such as gastropods a synthetic pesticide, tributyltin (TBT), was introduced and extensively used as a paint additive [1,2]. Its serious toxicity and hazard was later discovered and led to a recommendation by the International Maritime Organization to limit its application as an anti-fouling paint [3]. Today, TBT still contaminates many aquatic systems at various concentrations that cause adverse physiological effects in mammals and other organisms [4]. TBT is initially released into water, then partitioned and accumulated in soil and sediments [5]. The partitioning ratio of TBT in solid–water system is approximately 3:1 [6] which is moderately high compared with default model. The contaminant also accumulates in aquatic organisms due to the bioavailability of TBT in water media [7]. Accordingly, many researchers have focused on the impacts of TBT on living organisms, and also on effective options for TBT degradation. Photo-degradation is one of the techniques of interest for removing TBT from surface water and sediment utilising, UV and solar light radiation [8–11]. Previous work indicates that neither volatilization nor degradation of TBT species dissolved in water occurs over a period of 2 months in the dark at room temperature [8]. In sunlight, the compound undergoes slow photolytic decomposition with a half-life ($t_{1/2}$) > 89 days in water and about 120–150 days in water–sediment mixture [8]. Navio et al. reported the improvement of photo-degradation in a UV reactor that showed approximately an 80% reduction of TBT concentration in water within 30 h [9]. However, this efficient process is limited in the natural environment by the relatively lower intensity of UV in natural light [8]. Photocatalytic degradation is an alternative approach to enhance TBT degradation without the need for intense UV irradiation. Titanium dioxide is frequently used as a photocatalyst because of its availability, stability and low toxicity. In particular, the anatase form of TiO_2 has been utilized in many photo-degradation reactions: previous studies have focused on the degradation of toxic compounds such as bisphenol A, volatile organics and polycyclic aromatic hydrocarbons [12–14]. However, these is only one reported attempt at the photo-assisted degradation of butyltin in aqueous TiO_2 suspension (Degussa P25, 1–5 μm) calcined at 500 °C in an UV reactor. This achieved a 30% reduction in TBT concentration within 30 h [10,15]. The lower percentage degradation without catalyst might be due to the specific energy of the UV used in the reactor not being sufficient to generate electron–hole pairs from the catalyst, and the slightly large particle size of catalyst used.

The band gap energy of TiO_2 corresponds to the wavelength of UV light <400 nm [10,16]. Since sunlight consists mainly of visible

* Corresponding author at: David Livingstone Centre for Sustainability, Department of Civil Engineering, Faculty of Engineering, University of Strathclyde, Colville Building, Level 3, G4 ONG Glasgow, Scotland G1 1XN, United Kingdom.
Tel.: +44 0141 548 3161; fax: +44 0141 553 2066.
E-mail address: sornnarin.bangkedphol@strath.ac.uk (S. Bangkedphol).

0304-3894/$ – see front matter © 2010 Elsevier B.V. All rights reserved.
doi:10.1016/j.jhazmat.2010.08.068

wavelengths, these do not fit with TiO_2 band gap. This reduces the ability of TiO_2 to degrade toxic compounds under natural illumination. Consequently, the present study substituted some oxygen atoms of the TiO_2 with nitrogen atoms to improve the photo-degradation ability of the catalyst under natural conditions. The resulting mixed state of N_{2p} and O_{2p} lowers the band gap of TiO_2 so that irritations with sunlight can excite electrons from the valence band to the conduction band [17]. The photocatalytic mechanism of TiO_2 including N-doping involves creation of electron–hole pairs in the catalyst by light of energy higher than that of the band gap [18]. Some electrons are excited to the conduction band and holes remain in the valence band. Such holes act as a strong oxidizing agent, reacting with water molecules or hydroxyl groups on the catalyst surface to generate hydroxyl radicals ($^{\bullet}OH$), which initiate photo-degradation. Moreover, the excited electrons can also react with oxygen molecules to form superoxide radicals ($O_2^{\bullet -}$), which subsequently react with protons to produce hydroxyl radicals [19,20].

In this work, catalysts were prepared in the laboratory using a sol–gel method. This method is efficient for tailoring nanostructure materials with increased surface area of catalyst and that are simple to handle at room temperature [21]. This can improve the degradation ability of the catalyst under visible light and solar light [22]. The sol–gel preparation involves hydrolysis (A) and condensation (B) processes as follows:

$$(A) \equiv Ti{-}O{-}R + H{-}O{-}H \rightarrow \equiv Ti{-}O{-}H + R{-}O{-}H$$

$$(B) \equiv Ti{-}O{-}X + H{-}O{-}Ti\equiv \rightarrow \equiv Ti{-}O{-}Ti\equiv + X{-}O{-}H$$

where X is an alkyl group (R) or H.

Photocatalytic degradation of TBT upon N-doped TiO_2 under visible or natural light irradiation has not previously been reported in literature. Therefore, the main objective of this work was to study the enhancement of degradation of TBT, in visible and natural light, by nanoparticles of N-doped TiO_2 which have been prepared by the sol–gel method. The photo-activity of the synthesized catalyst was compared with those of undoped TiO_2 and P25–TiO_2, a standard commercial material for photocatalytic reactions, consists of 75% anatase and 25% rutile [23].

2. Materials and methods

2.1. Chemicals and instruments

The analytical standards used were tributyltin chloride (96% purity), dibutyltin chloride (98% purity), mono-butyltin chloride (95% purity) and tetrabutyltin obtained from Aldrich (Poole Dorset, UK). Ammonia solution (25%), tropolone (98% purity) and hexylmagnesium bromide solution (2 M in diethyl ether) were also obtained from Aldrich. Titanium (IV) tetraisopropoxide (AR grade) was obtained from ACROS (New Jersey, USA). Degussa P25 TiO_2 was obtained from S.M. Chemical (Bangkok, Thailand). Samples for X-ray powder diffraction (XRD) analysis were deposited on a silicon wafer sample holder and characterized using a Philips Pw 1830 X-ray diffractometer (Cu Kα, 1.5418 Å). Samples for transmission electron microscopy (TEM; JEOL 1200EX, 120 keV) were deposited on carbon-coated, 3-mm diameter, electron microscope grids. Percentage of nitrogen in the photocatalyst was determined by LECO CHNS-932 Elemental Analyzer using sulfamethazine as a standard material which consists of 51.78% C, 5.07% H, 20.13% N and 11.52% S. The GC–MS systems were a Hewlett-Packard 5980 gas chromatograph/quadrupole mass spectrometer (Ramsey, MN, USA) and a Thermo Scientific DSQ™ II single quadrupole GC–MS system (Loughborough, Leicestershire, UK).

2.2. Catalyst preparation

N-doped TiO_2 catalyst was prepared following the sol–gel method [20,24] by addition of 5 mL of 25% ammonia solution to 10 mL of titania precursor. In this work, titanium (IV) tetraisopropoxide was chosen as the main starting material because it is generally used for TiO_2 synthesis [25] and for commercial P25–TiO_2 [26,27].

After the reactions, the mixture was incubated at 30 °C for 1 h and then 105 °C for 1 h to obtain a pale yellow solid. Subsequently, the solid was calcined at temperatures between 300 and 600 °C for 1 h to provide catalysts for further characterization. The colour of catalysts varied depending on the calcination temperature, from brown at low temperature to white and light yellow at high temperature. Undoped TiO_2 was prepared under the same conditions as N-doped TiO_2 except that Nanopure water (resistivity less than 18 MΩ cm^{-1} at 25 °C) was added into the titania precursor instead of ammonia solution.

2.3. Photocatalytic degradation

Photocatalytic activity was assessed by the photo-degradation of TBT under artificial visible light and under natural light (in June 2009, Glasgow, UK). A stock solution of TBT 1000 μg mL^{-1} was prepared in methanol. From the stock solution, 10 μg mL^{-1} working solutions in nanopure water were freshly prepared prior to undertaking the reaction. The photocatalytic degradation was carried out in 250 mL beaker containing 150 mL working solution and 0.10 g of catalyst at room temperature (25–30 °C). For the visible irradiation, the reaction mixture was stirred for 30 min in the dark then stirred under visible light using a 190 W, Xe-lamp equipped with a HOYA UV 385 cut off filter at an average distance of 30 cm between water surface and lamp. Samples were collected between 30 min and 3 h. For the natural light, the reaction mixture was stirred in the dark for 30 min then stirred with direct exposure to sunlight. The experiments were carried out between 11:00 am and 5.00 pm during the months of June (summer season) in Glasgow (latitude: 55.8618, longitude: −4.2401). Samples were collected between 30 min and 5 h. Concentration of TBT and degradation products were determined in all samples using GC–MS. Dark control samples were covered with aluminum foil and stirred under the same condition.

2.4. Determination of tributyltin

The extraction was optimized as previously described [28]. A 15 mL aliquot of the sample solution was withdrawn from the beaker after switching off the stirrer for 5 min to allow settlement of catalyst. In triplicate, each 5 mL aliquot was adjusted to pH 1.7 and sodium chloride was added to 0.2% (w/v). Butyltins were extracted three times into hexane containing 0.05% tropolone, 10 mL of hexane in total, by shaking at 350 rpm for 30 min. All organic phases collected from each step were mixed and then evaporated until close to dryness on a heating block (20 °C) over N_2. A 0.25 mL internal standard, tetrabutyltin (1 μg mL^{-1}) in hexane was added to samples and volume was adjusted to 1 mL. Butyltins were derivatized with 0.5 mL 2 M *n*-hexylmagnesium bromide for 30 min under an inert atmosphere. 2 M HCl was then added to stop the reaction. Anhydrous ammonium sulfate was added to remove moisture. A 1 μL aliquot of solution was injected into the GC–MS with HP5-MS column (30 m × 0.25 mm i.d. × 0.25 μm). The carrier gas was helium at a flow rate of 1 mL min^{-1}. The injector and detector temperatures were held at 280 °C and 300 °C, respectively. The column oven temperature was programmed from an initial temperature of 100 °C, hold for 2 min, to a final temperature of 300 °C at the rate of 15 °C min^{-1}, and hold for 10 min. The peak areas and

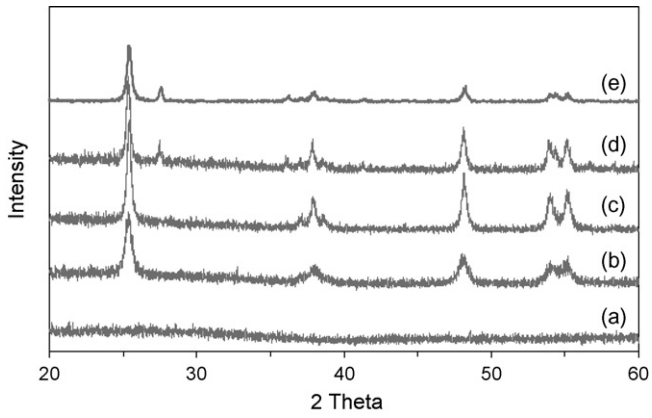

Fig. 1. XRD patterns of N-doped TiO_2 calcined at different temperatures. (a) 300 °C, (b) 400 °C, (c) 500 °C, (d) 600 °C and (e) P25–TiO_2.

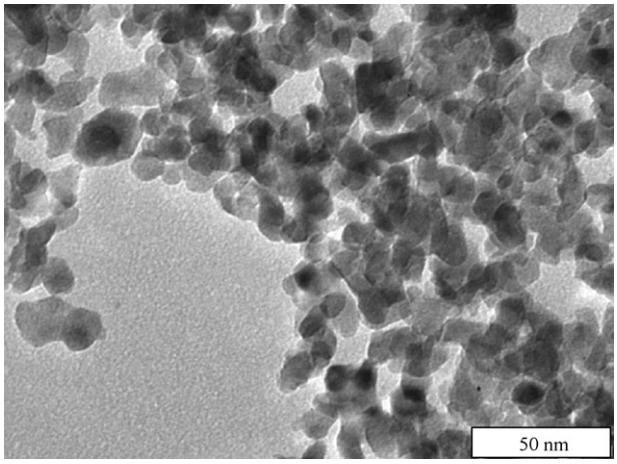

Fig. 2. TEM image of N-doped TiO_2 using titanium (IV) tetraisopropoxide as a titania precursor and calcined at 400 °C.

mass spectrum (Total Ion Chromatogram, TIC) were recorded. Calibration was performed in the range of 0.5–50 μg mL^{-1} for each butyltin.

3. Results and discussion

3.1. Characterization of catalyst

The X-ray diffractograms of N-doped TiO_2 calcined at differences temperature and P25–TiO_2 are presented in Fig. 1.

The XRD patterns in Fig. 1 exhibit amorphous, anatase and rutile phases, depending on the calcination temperature. At 300 °C (see (a)), no peaks occurred in the diffraction pattern, which indicates that the amorphous phase of N-doped TiO_2 was present. When the calcination temperature was raised to 400 °C, all peaks (2θ = 25.4°, 38.1°, 48.4°, 53.9°, 55.2°) which are regarded as an indicator of the anatase phase of titania were clearly observed. The crystalline anatase phase at a 2θ of 25.40° corresponding to the (1 0 1) reflection [29] started to appear at 400 °C and increased in intensity with increasing calcination temperature. When the calcination temperature was elevated to 600 °C, the transition to rutile phase could be observed. The characteristic peaks of rutile at a 2θ of 27.60° are corresponding to the (1 1 0) reflection [29] and at 36.1° [20,24] emerged.

The average particle size was calculated by applying Scherrer's equation to the anatase (1 0 1) and rutile (1 1 0) diffraction peaks which represented the highest intensity peak for each pure phase [30]. The percentage of anatase was calculated in accord with Spurr–Myers equation [31]. Unit cell volume was calculated from the product among three lattice parameters (a, b and c), which can be equated for the tetragonal system ($a \neq b$=c) [20]. The characterization results are shown in Table 1.

From the results, TiO_2 nanoparticles can be synthesized by the sol–gel process. Anatase has smaller crystallite size than rutile. The crystallite size represented specific surface area (m^2 g^{-1}) of catalyst which affects the photocatalytic activity. A small crystallite size has higher specific surface area than a larger crystallite. More surface area promotes greater efficiency on light and substance absorption on the surface, which increases the decomposition area and degradation activity of the catalyst [23]. The finding was supported by previous studies on photo-degradation of phenol and phenanthrene using difference particle sizes of N-doped TiO_2 [20]. The results showed that the smallest crystallite site of N-doped TiO_2 gave the greatest degradation. Moreover, N-doped TiO_2 calcined at 400 °C contains only anatase, which is reported to have higher photo-activity than rutile. The slow movement of electron in rutile provides more chances for electron–hole recombination and might cause this lower activity [32].

Therefore, N-doped TiO_2 calcined at 400 °C was chosen for the subsequent TBT degradation study. The photocatalytic efficiency of N-doped TiO_2 was compared to that in the absence of catalyst, and with those of commercial P25–TiO_2 and undoped TiO_2 synthesized by sol–gel method and calcined at 400 °C. The undoped TiO_2 crystalline was in anatase phase with a particle size of 11.3 nm and a unit cell volume of 0.133 nm^3. Additionally, the percentage of nitrogen in N-doped TiO_2 calcined at 400 °C was determined using an elemental analyzer. The result shows 0.054% ± 0.006 (n = 3) of nitrogen contained in doped catalyst, which is similar to previous studies depending on the titania precursor [20,22]. TEM photomicrograph of the N-doped TiO_2 confirmed the occurrence of spherical morphology nano-sized particles (Fig. 2).

Table 1
The effect of calcination temperature on the crystallite size, the content of anatase phase, unit cell volume and surface area of N-doped TiO_2 and P25–TiO_2.

Calcination temperature (°C)	% Anatase and rutile[a] (relative)	Crystallite size[b] (nm)	Unit cell volume[c] (nm^3)
400	100 (A)	16.3 (A)	0.135
500	100 (A)	24.7 (A)	0.135
600	67.9 (A)	28.1 (A)	0.135
	32.1 (R)	51.1 (R)	0.0619
P25–TiO_2	74.9 (A)	22.6 (A)	0.135
	25.1 (R)	45.5 (R)	0.0623

[a] Calculated with Spurr–Myers equation [31]: $w_A = 1/((1 + 1.26(I_R/I_A)))$ where, w_A is the weight fraction of anatase; and I_R and I_A are the intensity of the diffraction peak of rutile and anatase.

[b] Calculated by Scherrer's equation [30]: $d = k\lambda/(\beta \cos\theta_B)$ where, d is the crystallite size (nm); k is the shape factor (0.9); λ is the wavelength of the X-ray radiation source (nm); β is the full width at half maximum intensity (radians); and θ_B is Bragg angle.

[c] Calculated by [20]: $1/d^2 = ((h^2 + k^2)/a^2) + (l^2/c^2)$ where d is a lattice spacing; h, k, l are Miller indices; and a, b, c are lattice parameters.

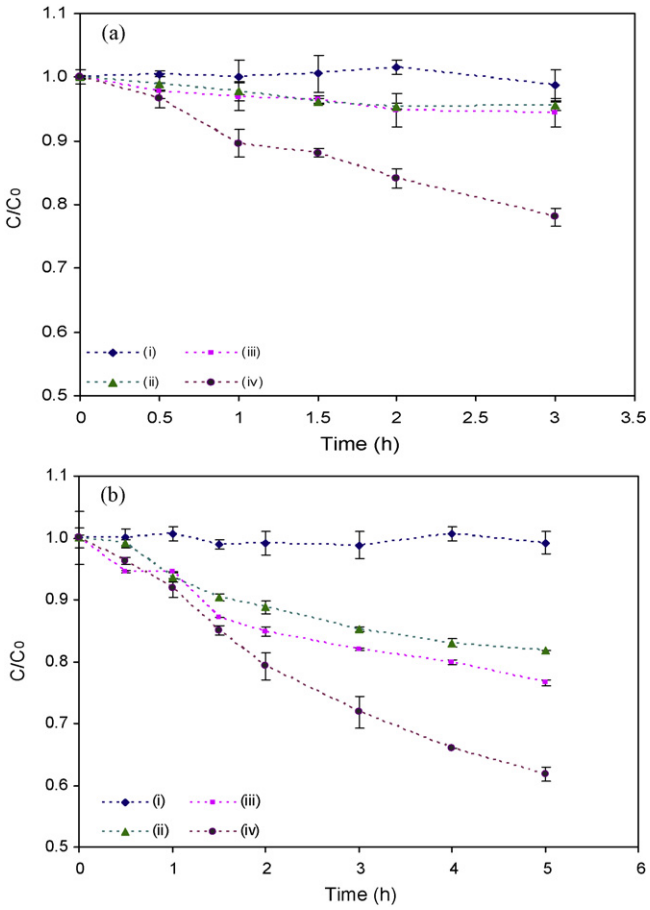

Fig. 3. Photo-degradation of TBT under visible light (a) and solar light (b) by (i) no catalyst, (ii) undoped TiO_2 calcined at 400 °C, (iii) P25–TiO_2 and (iv) N-doped TiO_2 calcined at 400 °C. Error bars represent one standard deviation for $n = 3$.

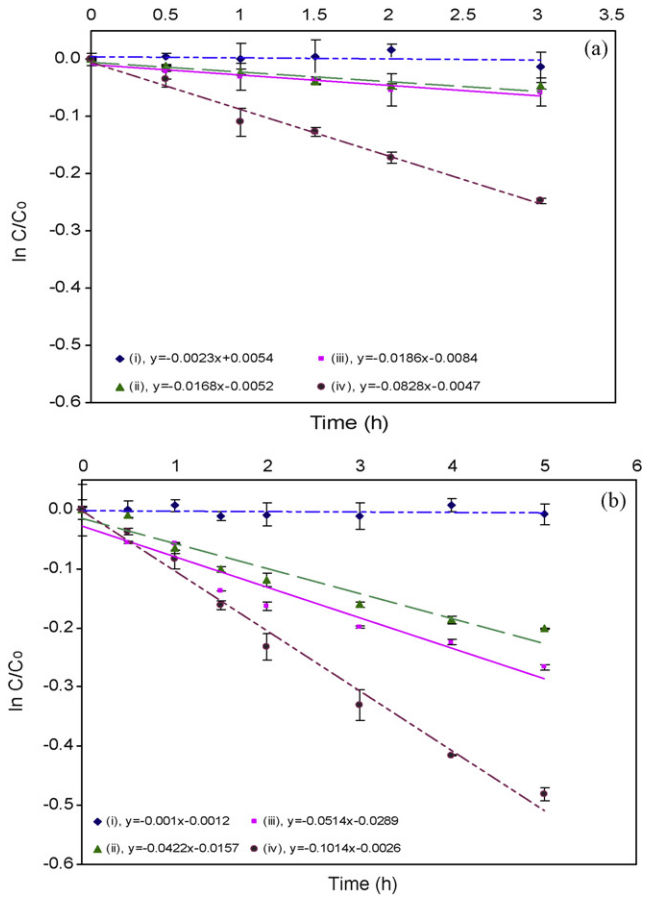

Fig. 4. The relation between ln C/C_0 and time (h) of TBT photo-degradation reaction under visible light (a) and solar light (b) by (i) no catalyst, (ii) undoped TiO_2 calcined at 400 °C, (iii) P25–TiO_2 and (iv) N-doped TiO_2 calcined at 400 °C.

3.2. Photocatalytic activity

Investigation of photocatalytic TBT degradation by the catalysts was performed under artificial visible light and natural light (Fig. 3). The photocatalytic efficiency was determined by calculating the relative concentration (C/C_0), where C is the concentration at the sampling time and C_0 is the initial concentration.

The N-doped TiO_2 calcined at 400 °C shows the highest efficiency whereas TBT concentration was not significantly changed in the absence of catalyst in both situations. Under visible light (Fig. 3a), undoped TiO_2 and P25–TiO_2 unsurprisingly demonstrated low degradation activity which corresponded with a previous study [10]. Since the band gaps energy of undoped TiO_2 and P25–TiO_2 are high (anatase and rutile are 3.2 and 3.0 eV, respectively), electron in the valence band cannot be excited to the conduction band by the low energy protons of visible light [16]. In natural light (Fig. 3b), the existence of UV wavelengths causes the degradation of TBT by undoped TiO_2 and P25–TiO_2. The higher degradation activity of P25–TiO_2 than undoped TiO_2 resulted from the developed crystallinity containing anatase and rutile (75:25). This prevents the recombination between holes and electrons [32] after "the line up of Fermi levels of anatase and rutile" [33]. The N-doped TiO_2 displayed successful degradation activity in natural light which is a result of "band gap narrowing" [17,34]. The degradation curves of TBT were well fitted by first order decay kinetics as presented in Fig. 4. In this experiment, the TBT degradation products, DBT and MBT species, could not be found in the reaction solution after irradiation. A high amount of N-doped TiO_2 catalyst and high conversion rate of DBT and MBT to final products such as carbon dioxide, water and inorganic tin species might explain this finding [10]. Indeed, the intermediates such as butanol, ethanol, hydroxylated di- and mono-butyltin [15] could be found by decreasing the amount of catalyst used. In addition, the photo-degradation mechanism of TBT by

Table 2
Reaction rate constants and % conversion of photocatalyst under artificial visible light and natural light.

Photocatalyst	Visible light			Natural light		
	% Conversion[a] (3 h)	R^2	Rate constant, k[b] (h^{-1})	% Conversion (3 h)	R^2	Rate constant, k (h^{-1})
No catalyst	1.20	0.071	ND[c]	1.16	0.049	ND
TiO_2	4.52	0.864	0.017	14.8	0.930	0.042
P25–TiO_2	5.54	0.906	0.019	18.0	0.932	0.051
N-doped TiO_2	21.9	0.983	0.083	28.2	0.987	0.101

[a] % Conversion was calculated from $(C_{initial} - C_{final}/C_{initial}) \times 100\%$.
[b] Rate constant was identified from slope of graph which presented the relation between ln C/C_0 and time (h), slope = $-k$.
[c] ND, non-detectable.

TiO_2 which was not different to N-doped TiO_2 has been presented by Navio et al. [10]. The rate constant of photocatalytic reaction was calculated from the slope of the first order reaction graph and % conversion of TBT after 3 h under visible light and natural light (Table 2).

Table 2, clearly confirms that N-doped TiO_2 has the highest photocatalytic ability to degrade TBT in water. Under natural light, 28% of TBT initially present is degraded in 3 h by the N-doped catalyst, and complete conversion would occur in 4–5 days depending on the weather. The advantages of catalytic photo-degradation of TBT in aqueous media when compared with biological process [35,36] are shorter degradation period, independence from microorganism behaviours and, especially, applicability at high TBT contamination levels. This process is an economically method in terms of catalyst preparation and natural light requirement, which can be applied for effective remediation of TBT in water.

4. Conclusions

A simple and economical sol–gel method was successfully applied for the synthesis of nanoparticle N-doped TiO_2, visible and natural light-active photocatalyst. According to XRD analysis, the N-doped TiO_2 transformed from anatase to rutile phase at calcination temperature ranging from 400 to 600 °C. Calcination of the doping catalyst at 400 °C was chosen. The N-doped catalyst enhanced the degradation of TBT in water under natural light, giving a 28% reduction in initial TBT concentration in 3 h. The process can now move forward to application on a larger scale for TBT remediation in water.

Acknowledgements

This work was partly supported by the Center for Innovation in Chemistry (PERCH-CIC), Commission on Higher Education, Ministry of Education, Thailand. We also acknowledge Assistant Professor Ekachai Hoonniwat for XRD facility.

References

[1] T.V. Hoang, A. Michel, A. Guyot, Polyvinylchloride stabilisation with organotin compounds—Part III: Effect of lewis acidity and co-ordination of organotin chlorides upon their catalytic activity towards dehydrochlorination, Degrad. Stabil. 4 (1982) 213–222.
[2] H. Rudel, Case study: bioavailability of tin and tin compounds, Ecotoxicol. Environ. Safe. 56 (2003) 180–189.
[3] International Maritime Organization, TBT Antifouling Ban: Account of Discussion at IMO-MEPC47, 2008, http://www.imo.org/.
[4] B. Antizar-Ladislao, Environmental levels, toxicity and human exposure to tributyltin (TBT)-contaminated marine environment: a review, Environ. Int. 34 (2008) 292–308.
[5] E.D. Burton, I.R. Phillips, D.W. Hawker, Sorption and desorption behavior of tributyltin with natural sediments, Environ. Sci. Technol. 38 (2004) 6694–6700.
[6] S. Bangkedphol, H. Keenan, C. Davidson, S. Sakultantimetha, A. Songsasen, The partition behavior of tributyltin and prediction of environmental fate, persistence and toxicity in aquatic environments, Chemosphere 77 (2009) 1326–1332.
[7] Extension Toxicology Network, Pesticide Information Profiles, 2009, http://extoxnet.orst.edu/pips/tributyl.htm.
[8] R.J. Maguire, A.J. Tkacz, Degradation of the tri-n-butyltin species in water and sediment from Toronto Harbour, J. Agric. Food Chem. 33 (1985) 947–953.
[9] J.A. Navio, F.J. Marchena, C. Cerrillos, F. Pablos, UV photolytic degradation of butyltin chlorides in water, J. Photochem. Photobiol. A 71 (1993) 97–102.
[10] J.A. Navio, C. Cerrillos, F.J. Marchena, F. Pablos, M.A. Pradera, Photoassisted degradation of n-butyltin chlorides in air-equilibrated aqueous TiO_2 suspension, Langmuir 12 (1996) 2007–2014.
[11] K. Saeki, A. Nabeshima, T. Kunito, Y. Oshima, The stability of butyltin compounds in a dredged heavily-contaminated sediment, Chemosphere 68 (2007) 1114–1119.
[12] S. Horikoshi, M. Kajitani, N. Serpone, The microwave-/photo-assisted degradation of bisphenol-A in aqueous TiO_2 dispersions revisited: re-assessment of the microwave non-thermal effect, J. Photochem. Photobiol. A 188 (2007) 1–4.
[13] D.S. Tsoukleris, T. Maggos, C. Vassilakos, P. Falaras, Photocatalytic degradation of volatile organics on TiO_2 embedded glass spherules, Catal. Today 129 (2007) 96–101.
[14] L.H. Zhang, P.J. Li, Z.Q. Gong, X.M. Li, Photocatalytic degradation of polycyclic aromatic hydrocarbons on soil surfaces using TiO_2 under UV light, J. Hazard. Mater. 158 (2008) 478–484.
[15] J.A. Navio, C. Cerrillos, M. Macias, Degradation of n-butyl tin chlorides in waters. A comparative assessment of the process by photo-assisted and chemical-treatment methods, J. Adv. Oxid. Technol. 12 (2009) 158–163.
[16] R. Nakamura, T. Tanaka, Y. Nakato, Mechanism for visible light responses in anodic photocurrents at N-doped TiO_2 film electrodes, J. Phys. Chem. B 108 (2004) 10617–10620.
[17] R. Asahi, T. Morikawa, T. Ohwaki, K. Aoki, Y. Taga, Visible-light photocatalysis in nitrogen-doped titanium oxides, Science 293 (2001) 269–271.
[18] H. Choi, E. Stathatos, D.D. Dionysiou, Sol–gel preparation of mesoporous photocatalytic TiO_2 films and TiO_2/Al_2O_3 composite membranes for environmental applications, Appl. Catal. B: Environ. 63 (2006) 60–67.
[19] P.C. Maness, S. Smolinski, D.M. Blake, Z. Huang, E.J. Wolfrum, W.A. Jacoby, Bactericidal activity of photocatalytic TiO_2 reaction: toward an understanding of its killing mechanism, Appl. Environ. Microb. 65 (1999) 4094–4098.
[20] W. Sirisaksoontorn, S. Thachepan, A. Songsasen, Photodegradation of phenanthrene by N-doped TiO_2 photocatalyst, J. Environ. Sci. Heal. A 44 (2009) 841–846.
[21] H. Shioji, S. Tsunoi, H. Harino, M. Tanaka, Liquid-phase microextraction of tributyltin and triphenyltin coupled with gas chromatography–tandem mass spectrometry—comparison between 4-fluorophenyl and ethyl derivatizations, J. Chromatogr. A 1048 (2004) 81–88.
[22] M. Ksibi, S. Rossignol, J.M. Tatibouet, C. Trapalis, Synthesis and solid characterization of nitrogen and sulfur-doped TiO_2 photocatalysts active under near visible light, Mater. Lett. 62 (2008) 4204–4206.
[23] T. Ohno, K. Sarukawa, K. Tokieda, M. Matsumura, Morphology of a TiO_2 photocatalyst (Degussa, P-25) consisting of anatase and rutile crystalline phases, J. Catal. 203 (2001) 82–86.
[24] Z.P. Wang, W.M. Cai, X.T. Hong, X.L. Zhao, F. Xu, C.G. Cai, Photocatalytic degradation of phenol in aqueous nitrogen-doped TiO_2 suspensions with various light sources, Appl. Catal. B: Environ. 57 (2005) 223–231.
[25] S. Qourzal, A. Assabbane, Y. Ait-Ichou, Synthesis of TiO_2 via hydrolysis of titanium tetraisopropoxide and its photocatalytic activity on a suspended mixture with activated carbon in the degradation of 2-naphthol, J. Photochem. Photobiol. A 163 (2004) 317–321.
[26] G. Sivalingam, K. Nagaveni, M.S. Hegde, G. Madras, Photocatalytic degradation of various dyes by combustion synthesized nano anatase TiO_2, Appl. Catal. B: Environ. 45 (2003) 23–38.
[27] K. Nagaveni, G. Sivalingam, M.S. Hedge, G. Madras, Solar photocatalytic degradation of dyes: high activity of combustion synthesized nano TiO_2, Appl. Catal. B: Environ. 48 (2004) 83–93.
[28] S. Bangkedphol, H. Keenan, C. Davidson, S. Sakultantimetha, A. Songsasen, Development of a low-cost method of analysis for the qualitative and quantitative analysis of butyltins in environmental samples, J. Environ. Sci. Heal. A 43 (2008) 1744–1751.
[29] Y. Nakano, T. Morikawa, T. Ohwaki, Y. Taga, Origin of visible-light sensitivity in N-doped TiO_2 films, Chem. Phys. 339 (2007) 20–26.
[30] A. Vomvas, K. Pomoni, C. Trapalis, N. Todorova, Photoconductivity in sol–gel TiO_2 thin films with and without ammonia treatment, Mater. Sci. 25 (2007) 809–816.
[31] R.A. Spurr, H. Myers, Quantitative analysis of anatase–rutile mixtures with an X-ray diffractometer, Anal. Chem. 29 (1957) 760–762.
[32] D.C. Hurum, K.A. Gray, T. Rajh, M.C. Thurnauer, Recombination pathways in the Degussa P25 formulation of TiO_2: surface versus lattice mechanisms, J. Phys. Chem. B 109 (2005) 977–980.
[33] B. Sun, A.V. Vorontsov, P.G. Smirniotis, Role of platinum deposited on TiO_2 in phenol photocatalytic oxidation, Langmuir 19 (2003) 3151–3156.
[34] T. Morikawa, R. Asahi, T. Ohwaki, K. Aoki, Y. Taga, Band-gap narrowing of titanium dioxide by nitrogen doping, Jpn. J. Appl. Phys. 2 40 (2001) L561–L563.
[35] H. Harino, M. Fukushima, Y. Kurokawa, S. Kawai, Susceptibility of bacterial populations to organotin compounds and microbial degradation of organotin compounds in environmental water, Environ. Pollut. 98 (1997) 157–162.
[36] P. Bernat, J. Dlugonski, Acceleration of tributyltin chloride (TBT) degradation in liquid cultures of the filamentous fungus Cunninghamella elegans, Chemosphere 62 (2006) 3–8.